Building Performance Loss After Damaging Earthquakes: an Investigation Towards Reparability Decisions

Marco Gaetani d'Aragona
PhD Candidate, Department of Structures for Engineering and Architecture, University Federico II, Naples, Italy

Maria Polese
Assistant Professor, Department of Structures for Engineering and Architecture, University Federico II, Naples, Italy

Kenneth J. Elwood
Professor, Dept. of Civil and Environmental Engineering, UA., Aukland, New Zealand

Majid Baradaran Shoraka
Postdoctoral Fellow, Dept. of Civil Engineering, U.B.C., Vancouver, Canada

Andrea Prota
Associate Professor, Department of Structures for Engineering and Architecture, University Federico II, Naples, Italy

Gaetano Manfredi
Professor, Department of Structures for Engineering and Architecture, University Federico II, Naples, Italy

In the aftermath of damaging events, agreed and transparent policies should establish acceptable levels of safety, and facilitate decisions on appropriate course of action for specific buildings. A significant indicator for repair and/or upgrade decisions is the Performance Loss (PL), that is a measure of variation of building seismic capacity from intact to damaged state. However, it is not clear how to choose significant PL thresholds with regard to damage acceptability. This study investigates, by means of a detailed case study, the expected PL for increasing seismic demand and its relationship with varied building safety level. The response of an existing non-ductile reinforced concrete building is simulated using a finite element model that properly accounts for both flexural, shear and axial failure of members and simulates joints behavior. Different definitions of building collapse are introduced, and consistent assessment of building PL are performed. The study shows interesting relations between PL and building safety level for varying return period of the damaging earthquake, demonstrating its usability as a practical indicator for reparability.

1. INTRODUCTION

In FEMA 308 (1998) a Performance-Based Policy Framework (PBPF) was introduced that relies on performance index of the building in its intact and damaged state and on the relative PL as significant indicators for repair and/or upgrade decisions. However, it is not clear how to choose significant PL thresholds with regard to damage acceptability. Proposals for capacity loss thresholds were given in the San Francisco Building Code (CCSF, 2010), recently updated in (SF, 2012), but a clear justification for those suggestions is missing. In (Polese et al, 2015a, b) simplified tools to assess PL and repair costs for damaged buildings were presented. In (Polese et al., 2013) a first comparison of simplified (e.g. pushover based) and detailed (nonlinear time history) approaches for evaluation of PL was

performed, showing that simplified procedures may be applied with comparable level of approximation for intact and damaged structures. Despite that, there is still the need to further investigate on suitable PL thresholds, and additional detailed studies are required. Recent works (e.g. Réveillère et al., 2012;Rahunandan et al., 2014), addressed the aftershock collapse vulnerability of RC damaged buildings; those studies allow to evaluate the safety variation based on the knowledge of maximum transient or residual drift. On the other hand, a faster evaluation in the post-earthquake could be achieved if aftershock fragilities are derived depending on the intensity of the damaging earthquake; indeed the latter information, that corresponds to T_R in a given hazard area, is quickly available soon after the Mainshock (MS). This paper presents first results of a larger study finalized at the detailed assessment of expected safety variation and repair costs for buildings having sustained MS of given intensity (Gaetani d'Aragona, 2015). In particular, it focuses on the evaluation of building seismic safety decay after a MS associating it to building PL. Multiple damaging earthquake intensities, representative of specific Return Periods T_R for the studied site are considered. Applying Mainshock – Aftershock (MS-AS) earthquake sequences, AS fragilities are built and used to estimate the variation of collapse probability. An existing seven-story non-ductile reinforced concrete (RC) structure with moment-resisting frame is considered. The response of the building is simulated with a detailed 2D nonlinear multi-degree-of freedom (MDOF) model. The model properly account for cumulative damage due to multiple earthquakes through hysteretic rules, damage progress, as well as both shear and axial failure in structural members. In addition, the definition of collapse modes typical for non-ductile frames are considered.

Paragraph 1 introduces the concept of PL. In Section 2, the formulation of AS collapse fragilities conditioned to multiple T_R for the MS is presented. Section 3 introduces two different collapse modes that are typical for older RC buildings. Section 4 describes the case study application. Section 5 examines the Incremental Dynamic Analysis (IDA) procedure to obtain both intact and T_R-dependent fragility curves. Finally, Section 6 shows first results for the case study.

2. DEFINITION OF PERFORMANCE LOSS

The building capacity after an earthquake may be significantly reduced due to the spread of damage all over the building, while the probability of collapse increases. Seismic behavior of damaged buildings, and their relative seismic safety, may be suitably represented by their seismic capacity modified due to damage, the so-called REsidual Capacity REC (Bazzurro et al., 2004; Polese et al., 2012). REC can be defined as a parameter aimed at representing the building seismic capacity (up to collapse) in terms of a spectral quantity. In particular, REC_{Sa} of a building is defined as the smallest ground motion spectral acceleration (at period T_{eq}, of the Single Degree Of Freedom SDOF system equivalent to the real structure) corresponding to collapse state of the building.

A significant indicator for repair and/or upgrade decision, is the PL index. Considering the variation of REC for a structure that has sustained an earthquake with Return Period T_R PL may be expressed as in Eq.(1):

$$PL = 1 - \frac{REC_{Sa,TR}}{REC_{Sa,0}} \tag{1}$$

with $REC_{Sa,0}$ the capacity of the intact building in terms of spectral acceleration and $REC_{Sa,TR}$ the capacity of the MS-damaged structure. The estimation of REC_{Sa} for both intact and damaged structures via IDA, and the computation of PL, is addressed in Section 5.

3. DERIVATION OF T_R DEPENDENT AFTERSHOCK FRAGILITY CURVES

Starting from the initial damage state produced by a MS corresponding to a given T_R, T_R dependent collapse fragility functions can be built. Because the structure is subject to a series of consecutive events, cumulative damage is accounted for in the estimate of the collapse probability.

Considering a seismic sequence consisted of a pair of mainshock MS and the consecutive aftershock event AS, the aftershock collapse probability conditioned on the MS intensity $S_{a,MS}$ can be calculated by considering two mutually exclusive and collectively exhaustive events (Benjamin and Cornell 1970) defined as C and NC (Eq. (2)). C accounts for cases where collapse occurs due to the mainshock and NC accounts for cases where collapse does not take place due to the mainshock (see Ebrahimian et al. 2014 and Jalayer et al. 2011a,b for more details on this type of expansion based on the Total Probability Theorem). In Eq. (2) $S_{a,MS}$ is MS spectral acceleration corresponding to a specific T_R conditioned on the site hazard, the fundamental vibration period of the intact structure (T_1), and the critical damping ratio assumed; $S_{a,AS}$ is the AS spectral intensity at T_1 and $S^C_{a,AS}$ is the AS spectral intensity corresponding to collapse. Assuming an equal probability of occurrence for each MS, the term $P(NC|S_{a,MS})$ can be estimated as the number of NC-cases over the number of MS considered (N_{MS}), while $P(C|S_{a,MS})$ can be estimated as the number of C-cases over N_{MS} and $P(x \geq S^C_{a,AS}|S_{a,MS}, C) = 1$. Hence, the AS fragility can be interpreted, for each considered structure and T_R (corresponding to $S_{a,MS}$), as the sum of the mainshock collapse fragility (last term in Eq. (2)), and an inflating term (first term in (2)). $P(x \geq S^C_{a,AS} \mid S_{a,MS}, NC)$ is the collapse probability conditioned on MS intensity $S_{a,MS}$ and on NC and can be expanded as in Eq. (3). Eq. (3) $\underline{MS}$ stands for the mainshock wave-form vector; $f(\underline{MS} \mid S_{a,MS}, NC)$ is the joint probability density function for the mainshock wave-form vector given a specific value for $S_{a,AS}$ and given NC.

The integral in Eq. (3) is an application of the Total Probability Theorem in conditioning on all possible mainshock waveforms conditioned on a given spectral acceleration value. It should be noted that the approximation to the integral in Eq. (3) is based on the assumption that the various mainshock wave-forms have equal probability of occurrence (see Jalayer et al. 2012 for more detail on this kind of approximation).

4. APPLICATION TO AN EXISTING RC BUILDING

4.1. Description of the building structural model

The model frame chosen in this study is the perimeter moment resisting frame of the Van Nuys Holiday Inn, that is a seven-story non-ductile reinforced concrete frame building located in Los Angeles, California, already described in (Krawinkler, 2005).

A fixed-base two-dimensional finite element MDOF model developed using OpenSees (2014) is adopted to simulate the seismic response of the building. The frame elements are modeled using the force-based nonlinear beam-column element with distributed nonlinear fiber sections (de Souza, 2000). The joint behavior is modeled using Alath and Kunnath (1995) model, which includes the pinching hysteretic behavior to account for the nonlinear shear deformation of the joint. The model does not account for axial failure of joints. Shear and axial failure in the columns are modeled using the Limit State material model (Elwood, 2004). P-Δ effects are included. A schematic view of the adopted numerical model is shown in Figure 1.

The eigenvalue analysis of the intact structure provides a fundamental vibration period of 1.0 sec.

$$P(x \geq S^C_{a,AS}|S_{a,MS}) = P(x \geq S^C_{a,AS}|S_{a,MS}, NC) \cdot P(NC|S_{a,MS}) + P(x \geq S^C_{a,AS}|S_{a,MS}, C) \cdot P(C|S_{a,MS}) \quad (2)$$

$$P(x \geq S^C_{a,AS}|S_{a,MS}, NC) = \int_{\forall \underline{MS}} P(x \geq S^C_{a,AS}|\underline{MS}, S_{a,MS}, NC) \cdot f(\underline{MS}|S_{a,MS}, NC) dMS \approx$$

$$\approx \frac{1}{N_{NC}} \sum_{i=1}^{N_{NC}} P(x \geq S^C_{a,AS}|\underline{MS_i}, S_{a,MS}, NC) \quad (3)$$

A damping of 2% is assigned to the first and third modes using Rayleigh damping. The damping is updated during the first-to-second earthquake analysis at the beginning of each seismic sequence, accounting for the first mode period elongation due to structural damage.

4.2. Ground motions selection

A set of 31 ground motions is selected from the PEER Next Generation Attenuation (NGA) database (2010). To reflect shaking intensity at site, ground motions have been selected using a target $\varepsilon(T_1)$ for the 2475 years return period. Ground motions MS-AS sequences are generated using this ground motions set where single earthquakes are applied as both MSs and ASs.

These 31 ground motions have M_w between 6 and 7.6, a closest distance from fault rupture between 7.1 and 48 km and a PGA varying between 0.105g and 0.82g. For further information on selection of accelerograms, refer to Baradaran Shoraka et al. (2013).

5. COLLAPSE SIMULATION

Older RC structures, non-conforming to modern design standards, are likely to experience gravity load collapse prior to side-sway collapse (Elwood et al., 2012). For this reason, this study considers two possible collapse mechanisms to capture the actual capacity in the model, as firstly proposed in Baradaran Shoraka et al. (2013): Side-sway collapse (SC) and Gravity load collapse (GLC). The SC occurs when a single storey has reached its capacity to withstand lateral loads (i.e., when every column in a given floor has exceeded its residual shear capacity at the same time). GLC occurs when vertical load demand exceeds the total vertical load capacity at a given storey. Collapse is detected based on a comparison of storey-level gravity load demands and capacities (adjusted at each time step to account for member damage and load redistribution).

The gravity load demand is considered constant during each analysis.

An internal algorithm monitors the dynamically varying capacity of each element and checks the GLC and SSC criteria throughout each nonlinear time history analysis to detect the collapse. A bisection algorithm is then implemented to find the collapse capacity with a precision of 0.05g during the IDA procedure. The collapse is considered as the first between GLC and SSC.

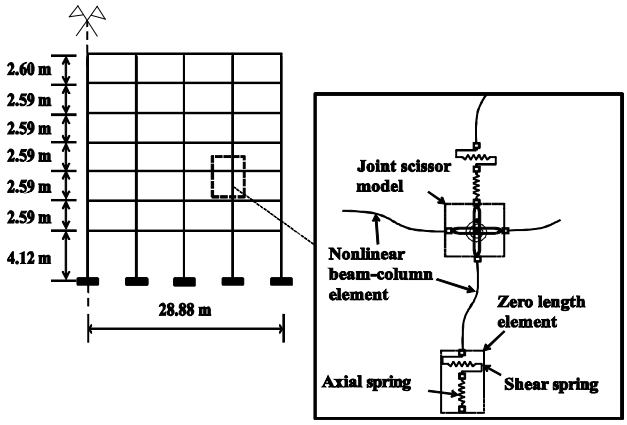

Figure 1: South frame elevation and column, beam and joint models (adapted from (Krawinkler, 2005))

6. INCREMENTAL DYNAMIC ANALYSES

The fragility computation is based on the use of IDA analyses (Vamvatsikos and Cornell, 2002), scaled up until collapse is reached; $S_a(T_1)$ is assumed as representative earthquake intensity.

To quantify structural response of the intact building, IDA is carried out on the nonlinear model of undamaged building using the set of 31 ground motions acting as MS. Residual capacity for each MS is calculated as the spectral intensity corresponding to the attainment of structural collapse (as defined in previous section); also, median REC is determined as the median spectral intensity over all MSs.

In order to evaluate AS fragilities, multiple earthquake sequences MS-AS are built through suitable scaling of selected accelerograms (see e.g. Figure 2). In particular, the MS record is scaled to represent different Return Periods for the specific area and structure. For the Los Angeles Area and a T_1=1.0 sec, the de-aggregation of seismic hazard provides $S_{a.MS}$ values of 0.29, 0.49, 0.65, 0.82 and 1.06g corresponding to the considered T_R = 72, 224, 475, 975, 2475 years respectively (http://geohazards.usgs.gov). For each (scaled) MS nonlinear time history is

performed and the response is recorded; then an AS record is applied to the MS-damaged structure. A time gap of 10 seconds between MS and AS is considered to allow the ceasing of vibration produced by the MS. Dynamic AS analysis is repeated with increasing scale factor applied to the AS record, providing IDA analysis results for MS-damaged structure, until the MS-AS sequence causes collapse. To account for the effect of record-to-record variability on structural response MS-AS sequences are generated using a set of 31 ground motions that are applied as both MSs and ASs, generating a total of 961 record sequences for each Return period.

The results show that in the majority of cases a first floor mechanism is activated due to the sole MS ground motion; also, usually the Gravity load collapse precede the Sidesway collapse. The type of mechanism usually does not change when considering the MS-AS sequence with the same MS, this may be attributed to the fact that the damage produced in the building by the MS, especially for higher Return Periods, may significantly affect the future collapse mechanisms that can develop in the building for ASs.

IDA is carried out on more than 4800 MS-AS sequences (961 MS-AS sequence for 5 Return periods). The process is computationally intensive, due to the use of a fiber model coupled with the Limit State Material, that allows to account for both shear and axial failure and load redistribution. In order to speed the analyses, OpenSees parallel (OpenSees, 2014) was used on SCoPE grid at the University of Naples Federico II. Running the analysis on the SCoPE grid in parallel reduces the computation to about 7 days with respect to 240 days required on a desktop computer with 4 processors. results and discussion

The REC of MS-damaged building is computed in terms of S_a based on the IDA results obtained from MS-AS sequences. The results are here represented in terms of fragility curve at collapse. For the undamaged building, the collapse fragility curve is based on the IDA results performed on the intact building using the set of 31 ground motions. The collapse fragility curve for damaged building is calculated based on the AS collapse capacities obtained for each of 961 MS-AS sequences in which the MS is scaled in order to be representative of the T_R of interest. Figure 3 illustrates the collapse fragility curves for the intact and damaged building in terms of probability of collapse conditioned on the MS for given T_R as a function of AS spectral intensity, $S_{a,AS}(T_1)$. The red curve represents the behavior of the intact building. As the T_R increases, due to the increasing building damage for MS application, the collapse fragility curve shift left and up. Because for increasing T_R an increasing number of collapses due to MS is detected, the collapse fragility curves for higher T_R have nonzero probability of collapse for $S_{a,AS}$=0.

A comprehensive indicator of the structural safety that involves considering both the hazard curve at the site and the collapse fragility curves is the probability of collapse over *t* years.

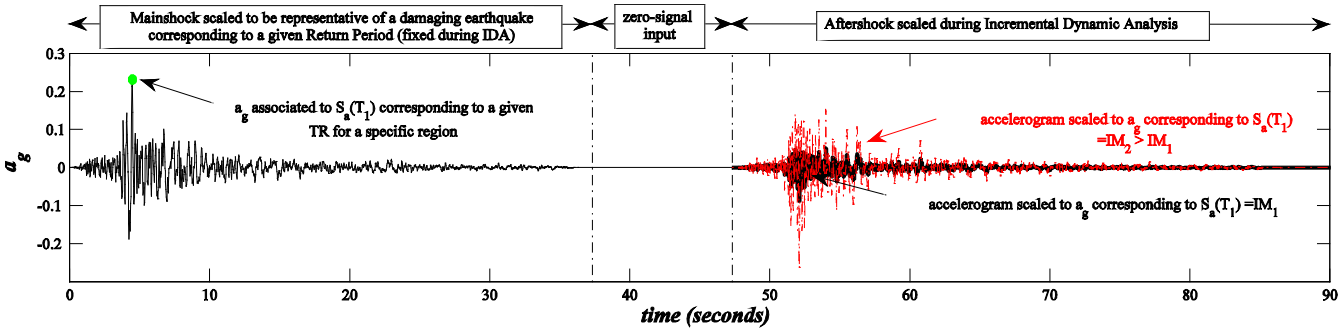

Figure 2: Example of Mainshock-Aftershock sequence

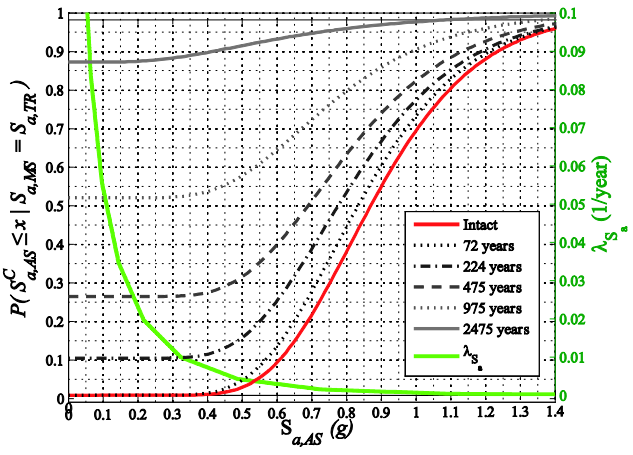

Figure 3: T_R-dependent fragilities at collapse

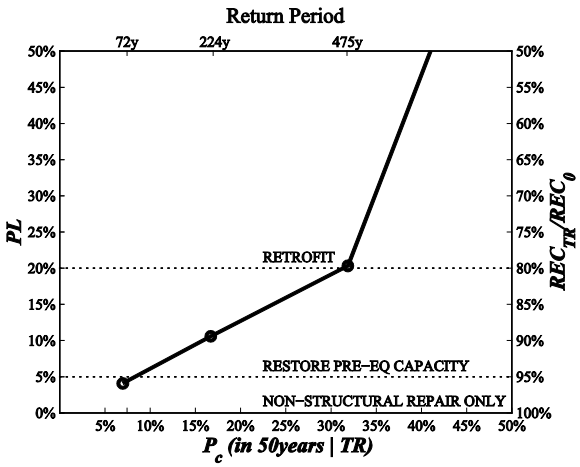

Figure 4: Relations between T_R, P_C in 50 years conditioned to T_R, PL and REC variation.

Under the hypothesis that the occurrence of earthquakes in time follows a Poisson process, the probability of one collapse over *t* years can be computed as:

$$P_c(\text{in } t \text{ years}) = 1 - \exp(-\lambda_c t) \quad (4)$$

with λ_c the mean annual frequency of collapse. λ_c can be calculated integrating the collapse fragility curve of the structure over the seismic hazard curve (Figure 3) at the site using the relation $\lambda_c = \int_0^\infty P(C|im)|d\lambda_{IM}(im)|$ (Eads et al. 2013), where P(C|im) is the probability that the structure will collapse when subjected to an earthquake with ground motion intensity level *im*, and λ_{IM} is the mean annual frequency of exceedance of the ground motion intensity *im*. In order to account for the possibility that the MS caused collapse, the Eq.(4) can be rewritten using the Total Probability Theorem by separating C and NC cases for a given T_R.

The "degraded" REC_{TR}, corresponding to each return period, is computed as the median collapse capacity from the Aftershock IDA analyses. Then, the corresponding PL is calculated with Eq. (1). Figure 4 shows the relation between PL, REC, T_R and the probability of collapse in a time window of 50 years.

Note that in more than 50% of cases for $T_R \ge$ 975 years collapse occurs due to the MS, with a median value of PL corresponding to 100% (not shown in figure); obviously, in calculating collapse probability the entire fragility is taken into account, resulting in different (increasing) P_C (in 50 years) for T_R 975 (56%) and 2475 (90%). As expected, for increasing T_R the probability of collapse increases. The same trend is observed for PL, while the ratio REC_{TR}/REC_0 decreases.

The median probability of collapse in 50 years is 6.1% for the intact building while it increases to 7.0% for a 72-years-MS-damaged structure and up to a maximum value of 89.6% when considering a Return Period of 2475 years. In the same figure the restore and retrofit trigger values in terms of PL, as suggested in (SF, 2012) and considering that for Van Nuys site $S_{a,0.3} \ge 0.4$g for any Return Period are shown.

Other remarkable observation concern the variation in the fundamental vibration period (T_1), which is strictly related to the global damage (Di Pasquale et al., 1990). The median variation of the fundamental vibration period with respect to the one for intact building varies with T_R. These values vary in a non-linear way, from a minimum of 0.5% for 72 years return period up to 21% for the 2475 years return period. The same trend is observable for the maximum interstorey drift ratio: the median for T_R=72 years is 0.9% and increases up to 3.7% for T_R=2475 years.

Another interesting parameter is the maximum residual drift, that is often used as limit for technical feasibility of repair intervention and

is a directly measurable damage indicator. Its median values vary with T_R from a minimum of 0.02% for T_R=72 years up to 0.46% for T_R=2475 years.

7. CONCLUSIONS

The study presented in this paper aimed at contributing to quantification of PL thresholds to facilitate the repair and/or upgrade decision process after a damaging earthquake. In particular, the PL index was computed with reference to five different Return Periods, via Incremental Dynamic Analysis, for an existing non-ductile seven-story building in the Los Angeles area.

The response of the building was simulated by means of a detailed 2D nonlinear multi-degree-of freedom (MDOF) finite element model. The model properly account for brittle failures and captures typical non-ductile RC frames failure modes.

The analytical model of building was subjected to multiple sequences comprised of two recorded ground motions to simulate the damage produced on the building by a MS of a given Return Period.

The results show that the REsidual Capacity REC of a MS-damaged building may be significantly smaller (PL higher) than the REC of an intact building. However, for a MS with a T_R = 72 years the building capacity is only slightly affected. For increasing T_R, the PL increases very fast up to the 100% for MS corresponding to T_R = 975 years. For T_R 975 years or larger, the number of collapse cases due to MS becomes greater than the non-collapse cases, and the median capacity becomes zero.

Previous studies (Rahunandan et al., 2014) highlighted that the polarity of the second earthquake may affect the behavior of the building and vary the collapse capacity. However, in this study the effect of polarity on REC has been neglected and has to be properly taken into account in future works.

The establishment of PL thresholds that trigger a specific intervention on a damaged building cannot exclude consideration about repair/retrofit costs associated with a MS ground motion.

Further studies are required to assess these thresholds conduced on a larger building inventory, in order to suggest a comprehensive and uniformly applicable post-earthquake repair framework, that includes economic loss estimate coupled with variation of post-earthquake seismic safety.

8. AKNOWLEDGEMENTS

This study was performed in the framework of PE 2014–2016; joint program DPC-Reluis Task 3.3: Reparability limit state and damage cumulated effects and Task 3.5 Methods for the definition of thresholds for seismic retrofit. The S.Co.P.E. computing infrastructure at the University of Naples Federico II was used for parallel computing.

9. REFERENCES

Alath, S., Kunnath, S.K. (1995). “Modeling inelastic shear deformation in RC beam-column joints”. *Engineering Mechanics Proceedings of 10th Conference*, May 21-24, ASCE, Boulder, CO, USA, 1995; 822–825.

Baradaran Shoraka, M., Yang, T.Y., Elwood, K.J, (2013). “Seismic Loss estimation of non-ductile reinforced concrete buildings”, *Earthquake Engng Struct. Dyn*, 42, 297-310.

Bazzurro P, Cornell C A, Menun C, Motahari M (2004) “Guidelines for seismic assessment of damaged buildings”, *13WCEE* Vancouver, B.C., Canada, 2004. Paper No. 1708.

Benjamin, J.R., Cornell, C. A. (1970). “Probability, statistics and decision for civil engineers”, McGraw-Hill.

de Souza, R.M. (2000). “Force-based finite element for large displacement inelastic analysis of frames”. PhD thesis, University of California, Berkeley, United States, California.

Di Pasquale, E., Ju, J. W., Askar, A., & Çakmak, A. S. (1990). “Relation between global damage indices and local stiffness degradation” *Journal of Structural Engineering*, 116(5), 1440-1456.

Eads, L., Miranda, E., Krawinkler, H., & Lignos, D. G. (2013). “An efficient method for estimating the collapse risk of structures in seismic

regions" *Earthquake Engng Struct. Dyn*, 42(1), 25-41.

Ebrahimian, H, Jalayer, F, Asprone, D, Lombardi, AM, Marzocchi, W, Prota, A, Manfredi, G. (2014) "A Performance-based Framework for Adaptive Seismic Aftershock Risk Assessment" *Earthquake Engng Struct. Dyn*, Volume 43, Issue 14, pages 2179–2197

Elwood, K.J. (2004). "Modelling failures in existing reinforced concrete columns". *Canadian Journal of Civil Engineering*; 31(5): 846–859.

Elwood, K.J., Holmes, W.T., Comartin, C.D., Heintz, C., Rojahn, C., Dragovich, J., McCabe, S., Mahoney, M. (2012). "Collapse Assessment and Mitigation of Nonductile Concrete Buildings: ATC-76-5/ATC-78/ATC-95". 15WCEE, Lisbon, Portugal, 24–28 Sept.

FEMA 308 (1998). "Repair of earthquake damaged concrete and masonry wall buildings". Federal Emergency Management Agency. Washington D.C.

Gaetani d'Aragona, M., (2015) "Post-Earthquake Assessment of Damaged non-Ductile Buildings: Detailed Evaluation for Rational Reparability Decisions", PhD Thesis, University of Naples Federico II, Italy

Jalayer, F., Beck, J.L., Zareian, F. (2012). "Intensity Measures of Ground Shaking Based on Information Theory'', *Journal of Engineering Mechanics*, 138 (3) , pp. 307-316.

Jalayer, F., Asprone, D., Prota, A., Manfredi, G. (2011a) "A decision support system for post-earthquake reliability assessment of structures subjected to after-shocks: an application to L'Aquila earthquake, 2009", *Bull Earthquake Eng*, 9 (4) , pp. 997-1014.

Jalayer F., Asprone D., Prota A., Manfredi G. (2011b). "Multi-Hazard Upgrade Decision-Making for Critical Infrastructure based on Life Cycle Cost Criteria", *Earthquake Engng Struct. Dyn*, 40 (10) , pp. 1163-1179.

Krawinkler, H. (2005). "Van Nuys Hotel Building Testbed Report: Exercising Seismic Performance Assessment". PEER Report 2005/11. College of Engineering, University of California, Berkeley.

OpenSees (2014). "Open system for earthquake engineering simulation OpenSees framework-Version 2.4.4. Pacific Earthquake Engineering Research Center, Univ. of California, Berkeley.

Pacific Earthquake Engineering Research Center (PEER). PEER NGA database flatfile. (2010). <http://peer.berkeley.edu/nga/flatfile.html> [10 September 2010].

Polese, M., Di Ludovico, M., Prota, A., Manfredi, G. (2012). "Damage-dependent vulnerability curves for existing buildings". *Earthquake Engng Struct. Dyn*, 42 (6), 853-870, DOI: 10.1002/eqe.2249.

Polese, M., Gaetani d'Aragona, M., Prota, A., Manfredi, G. (2013). "Seismic behavior of damaged buildings: a comparison of static and dynamic nonlinear approach", paper # 1134, proc. of *COMPDYN 2013*, Kos Island, Greece, 12–14 June 2013.

Polese, M., Di Ludovico, M., Marcolini, M., Prota, A., Manfredi, G., (2015a) "Assessing reparability: simple tools for estimation of costs and performance loss of earthquake damaged r.c. buildings", *Earthquake Engng Struct. Dyn*, in press, DOI: 10.1002/eqe.2534.

Polese M, Marcolini M, Zuccaro G, Cacace F (2015b) Mechanism Based Assessment of Damaged-Dependent Fragility curves for RC building classes, *Bull Earthquake Eng*, in press, DOI 10.1007/s10518-014-9663-4

San Francisco, City of (SF), (2012) "Post-earthquake repair and Retrofit Requirements", Administrative Bulletins, AB-099, Department of Building Inspection, San Francisco, CA

Rahunandan, M., Liel, A.B., Luco, N., (2014). "Aftershock collapse vulnerability assessment of reinforced concrete frame structures", *Earthquake Engng Struct. Dyn*; DOI: 10.1002/eqe.2478

Réveillère, A., Gehl, P., Seyedi, D., Modaressi, H., (2012) "Development of seismic fragility curves for damaged reinforced concrete structures", 15WCEE, Lisbon, Portugal, 24–28 Sept.

Vamvatsikos D, Cornell A (2002) "Incremental dynamic analysis". *Earthquake Engng Struct. Dyn*; 31 (3): 491-5.